Journal of Catalysis 319 (2014) 110–118

Contents lists available at ScienceDirect

Journal of Catalysis

journal homepage: www.elsevier.com/locate/jcat

SiO_2-, Cu-, and Ni-supported Au nanoparticles for selective glycerol oxidation in the liquid phase

Maciej Kapkowski [a], Piotr Bartczak [a,d], Mateusz Korzec [a], Rafal Sitko [a], Jacek Szade [b], Katarzyna Balin [b], Józef Lelątko [c], Jaroslaw Polanski [a,*]

[a] Institute of Chemistry, University of Silesia, Szkolna 9, 40-006 Katowice, Poland
[b] Chełkowski Institute of Physics, ul. Uniwersytecka 4, 40-007 Katowice, Poland
[c] Institute of Materials Science, University of Silesia, 75 Pułku Piechoty 1A, 41-500 Chorzów, Poland
[d] NANO-CHEM-TECH, Ligocka 90A/14, 40-568 Katowice, Poland

ARTICLE INFO

Article history:
Received 14 June 2014
Revised 6 August 2014
Accepted 6 August 2014

Keywords:
Au nanoparticles
Glycerol oxidation
Bimetallic Au/Cu
Au/Ni
Heterogeneous catalysis
Silica supported nanogold
Silica support

ABSTRACT

We tested for the first time the efficiency of SiO_2-, Cu-, and Ni-supported Au in deep glycerol oxidation in a diluted and viscous H_2O_2/H_2O liquid phase. Acetic acid (AA), the C_2 oxidate, was preferentially formed in such a system. High conversion (100%) and AA yields (90%) were observed for the sol–gel SiO_2-supported Au in diluted solutions. Although with the increase of glycerol concentration in the viscous liquid phase these values decreased to ca. 40% (conversion) and 20% (AA yield), the addition of acetonitrile improved the AA yield to ca. 40%, while the surfactants were found to be capable of a many-fold enhancement of the catalyst activity at the room temperature highly viscous liquid phase. High performances were also observed for the bimetallic Au/Cu and Au/Ni catalysts obtained by nano-Au transfer; however, these catalysts were destroyed during the reaction by the Cu or Ni leaching effect.

1. Introduction

Renewable naturally sourced carbohydrates, amino acids, and triglycerides are available in vast quantities in our environment. This biomass, a product of living organisms, could be used as valuable feedstock for chemical processing; however, we need *novel chemistry to transform large amounts selectively and efficiently in their natural state without extensive functionalization and protection* [1]. For this reason, biomass conversion has received increasing attention in contemporary chemistry. Glycerol yielded as a by-product in biodiesel production is one of the most widely-available biosourced chemicals, making it an attractive target of investigations. The oxidation of glycerol could yield a variety of C_1 to C_3 oxygenates, which are potentially valuable chemicals in chemical and pharmaceutical applications or intermediates in organic synthesis. This has triggered a growing interest in new methods for this process. Although there has been tremendous progress in recent years in this area, a number of problems remain to be solved [2,3]. Available enzymatic or stoichiometric methods are often wasteful and economically inefficient. Alternatively, a variety of catalytic reactions have been developed; e.g., catalytic glycerol conversions have been thoroughly reviewed [4]. Nanocatalysis is an interesting option in this area.

Nanocatalysts are extremely sensitive toward structure differentiation, and their activity and selectivity depend not only on nanometal and support type but also on size, shape, and composition [5]. Thus, optimization of such materials is an open issue. In fact, more efficient catalysts are still being sought to run the reactions with higher yields and higher selectivity under mild conditions. Other important problems to be addressed include reducing the fraction of noble metals, facilitating the catalyst separation, improving reusability, and reducing contamination of the final products. Gold nanoparticles (Au NPs) catalyze a variety of reactions [6–9]. As they tend to agglomerate, they are usually supported on carriers to form more stable catalytic systems. Generally, Au NPs are available on a variety of supports, from carbon-like graphite to inorganic materials. Basically, the first should be wettable by apolar reagents and solvents, while the latter should be wettable by polar ones. Wettability, and consequently catalyst availability for the reactants, is of crucial importance for the reaction progress; e.g., the recently oxidation of cyclohexene and D-glucose over nano-Au/SiO_2 in water has been compared. In this reaction, polar polyhydroxyl D-glucose complying with polar SiO_2

* Corresponding author.
E-mail address: polanski@us.edu.pl (J. Polanski).

http://dx.doi.org/10.1016/j.jcat.2014.08.003
0021-9517/

support and a polar solvent (H_2O) reacted smoothly at room temperature, whereas nonpolar cyclohexene violating the polarity rule needed the addition of surfactants to react efficiently [10].

Glycerol oxidation catalyzed on Au NPs, pioneered by Hutchings et al. [11,12], has been exhaustively studied recently [8,9,13–17]. Possible glycerol oxidates can be connected by a complex reaction network [3,16,21]. Scheme 1 presents a variety of products yielded from such catalytic systems, with nanometals supported on carbon or inorganic carriers. The C_3 oxygenates, of which dihydroxyacetone is the most desired product, designate oxidation without C–C cleavage. Possible products and catalytic systems are specified in Tables 15 and 16 of Ref. [3]. In contrast, oxidation to C_2 has been investigated as a potential source of glycolic acid [18] and C_1 products. In turn, CO_2 and HCOOH are products of the highest chain decomposition level.

Glycerol oxidation by aqueous hydrogen peroxide in an autoclave reactor on Au/C, Au/graphite, or Au/TiO_2 under the presence of NaOH provided a mixture of glycolate, glycerate, and tartronate [18]. Moreover, oxidation of glycerol to glyceric acid using an Au/graphite system in aqueous sodium hydroxide under basic free [19] or mild conditions [11] also appeared to be relatively selective. The influence of various carbonaceous supporting materials on the Au/C catalyst performance in glycerol oxidation was described by Gil et al. [20]. More generally, the influence of various support materials on catalytic glycerol oxidation was reviewed by Katryniok et al. [16].

In this study, we tested the efficiency of the deep oxidation of glycerol in the presence of unmodified silica-supported nanogold catalyst in aqueous 30% hydrogen peroxide, under mild conditions in aqueous glycerol solutions of various dilutions. We assumed that polar glycerol or a glycerol/water mixture would prefer a relatively hydrophilic catalyst carrier, which should provide the widest wettability and availability for the reacting molecules. This would be especially important for highly viscous undiluted glycerol solutions. Thus, a suspension of the silica-supported catalyst should provide a system in which the reaction proceeds smoothly, while hydrogen peroxide could be a compatible convenient, safe, and green reagent in such a system. It is also a model oxidant, since it was reported that aerobic oxidation on Au NPs proceeds with in situ formation of H_2O_2 [16]. To the best of our knowledge, the oxidation of glycerol on SiO_2-supported nano-Au has never been investigated, despite the polarity match between glycerol, SiO_2, and H_2O_2/H_2O systems. Recently, we reported a new method for transferring SiO_2-supported nanometals to a variety of other supports [22]. As Au/Cu nanoparticles have been recently developed as an interesting catalyst for the oxidation of various alcohols [23], here we prepared bimetallic nano-Au supported on Cu or Ni grains, to test their performance in glycerol oxidation. Despite the complex network of possible reactions (Scheme 1), a process of deep glycerol oxidation proceeds on the investigated catalysts preferentially to acetic acid (AA).

2. Experimental

2.1. Preparation of Au NPs on silica or Cu and Ni carriers

The series of nanocatalysts, namely Au/silica or Au/Cu and Au/Ni were prepared according to the procedure optimized (for details see: Supplementary material).

2.2. Glycerol oxidation

Nano-Au catalyst (20 mg, 0.2–20.0 μmol Au) was suspended in a mixture of 1.0 mL of 30% hydrogen peroxide (10 mmol H_2O_2) and

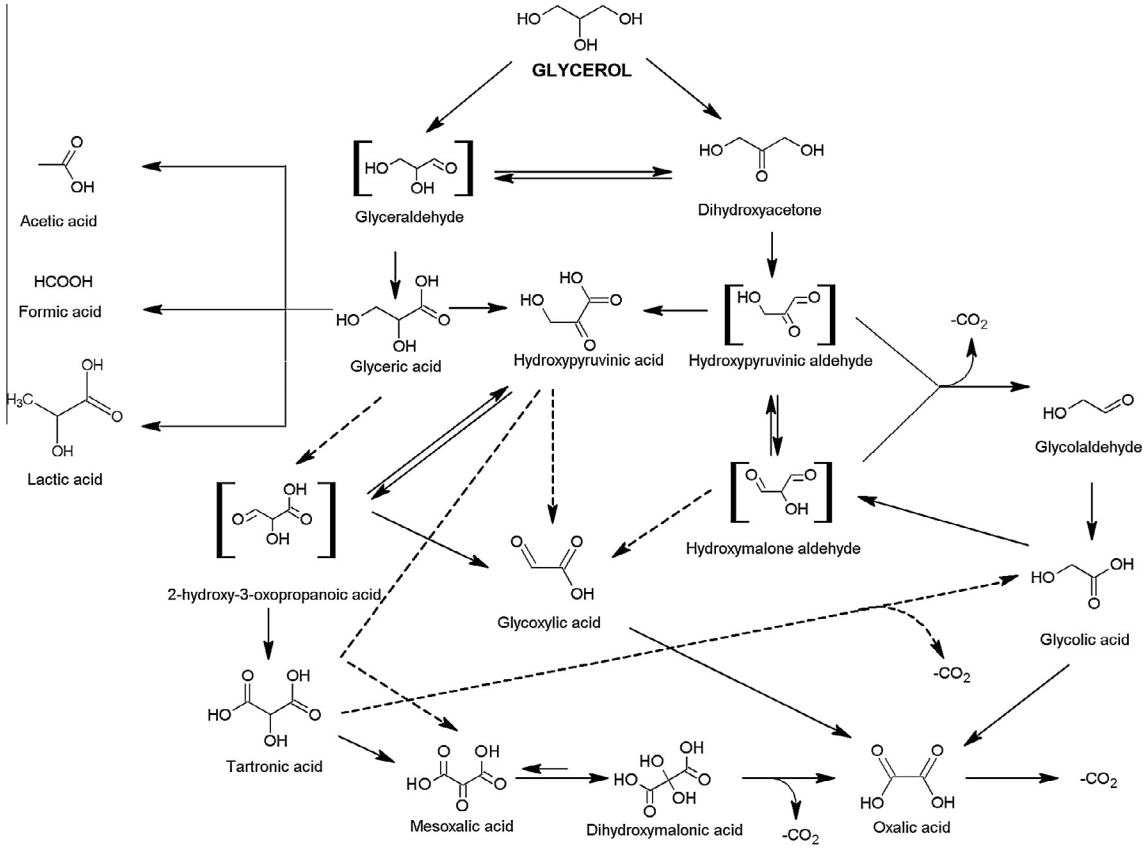

Scheme 1. A complex reaction network of glycerol oxidation [16].

0.5 mL (0.5–13.6 mol/L) glycerol (Fisher BioReagents® – Glycerol For Molecular Biology) by sonication at room temperature for 10 min (RK 52 H, Bandolin Electronics, 35 kHz). Reagents were stirred at 770 rpm in a sealed tube (septa system) placed in a thermostated oil bath at 80 °C for 24 h. The resulted reaction mixture was centrifuged and decantated. The supernatant was dissolved into deuterated water and analyzed using ^{1}H and ^{13}C NMR. For quantitative determination of the reaction products, we used an external standard procedure with Coaxial Small Volume NMR Insert tubes (ARMAR Chemicals) and hydroquinone as a reference substance. Additionally, the 2D COSY and HMQC methods were used to identify and quantify products. The spectra were recorded on the Bruker Avance 400 or 500 spectrometers with TMS as internal standard (400 MHz, ^{1}H, 101 MHz ^{13}C or 500 MHz, ^{1}H, 126 MHz ^{13}C) at room temperature. The signal from water was suppressed using 90 water-selective pulses (zggpwg). Optionally this oxidation procedure was modified by the addition of 1.0 mL acetonitrile (19.10 mmol) or surfactants: Sulforkanol (sodium laureth sulfate – SLES), Triton X-100, PEG 400, ca. (0.05 wt.%).

3. Results and discussion

A variety of nano-Au/C supported catalytic systems have been developed recently for the selective oxidation of glycerol [26]; however, there have been no reports on the possible application of SiO_2-supported Au NPs in glycerol processing. In turn, silica-supported Nb- and W-oxide, if applied to the gas phase dehydration of glycerol under argon, appeared to yield acrolein [27]. Recent developments in this field were discussed in [28]. Additionally, various mixed oxide catalysts were used in glycerol oxydehydration, another variant of catalytic glycerol processing that was also tested in the gas phase [29].

3.1. The catalysts preparation and structure

We used amorphous silica synthesized by the sol–gel [25] technique as a basic carrier. SEM observations indicated that silica obtained by this method exhibited a regular spherical shape, a controlled size distribution, and a uniform porous surface (Fig. S1, Supplementary material). This regular shape was preserved in Au NPs supported on the SiO_2 carrier obtained using the Stöber method [24].

The EDXRF spectrum of 0.1% Au/SiO_2, in contrast to SiO_2, shows several peaks at 8.45, 9.71, 10.26, 11.44, and 13.38 keV, which correspond to the Au lines Ll, Lα, Ln, Lβ, and Lγ, respectively (Fig. S2, Supplementary material). The quantitative EDXRF analysis reveals the presence of minor (Ca) and trace elements (Cr, Mn, Fe, Ni, Cu, and Pt), in both SiO_2 and Au/SiO_2 (for more details see Table S1, Supplementary material). The determined concentration of Au, 0.092%, is very close to the designed and expected value of 0.1% (Table 1, entry 2). In contrast, the XPS analysis, if used to determine the Au concentration on the catalyst surface, indicated entirely different values. For the 0.1% Au supported on sol–gel, SiO_2 surface Au concentrations determined by XPS are lower than those determined by EDXRF. This suggests that in the 0.1% Au/SiO_2 catalyst, in addition to the Au NPs located directly on the catalyst surface, some of their important parts are located within SiO_2 pores that are out of view of the XPS analysis. It should be noted that X-rays have a much larger penetration range compared to silica particles. The information depth $d_{99\%}$ for any element that yields 99% of the element intensity is given by the formula $d_{99\%} = 4.6/\chi(E_0,E_i) \times \rho$, where ρ is the density of the sample and $\chi(E_0,E_i) = \mu(E_0)\csc(\phi_1) + \mu(E_i)\csc(\phi_2)$ is the total mass-attenuation coefficient of the sample. $\mu(E_0)$ and $\mu(E_i)$ represent the mass attenuation coefficients of the sample at the primary E_0 and fluorescent radiation E_i (analytical line of Au, i.e., Lα at 9.71 keV), and ϕ_1 and ϕ_2 are the incidence and take-off angles, respectively. The information depth $d_{99\%}$ calculated for gold (Au Lα line) in silica particles is ca. 530 μm. This is much larger than the diameter of silica particles, i.e., 500–1200 nm. Therefore, in contrast to XPS results which reveal the surface structure of the samples, EDXRF provides us with the representative bulk composition of the catalysts.

Also, SEM and TEM analyses indicate that a surface texture of 0.1% Au/SiO_2 evidently differs from that of the higher Au content Au/SiO_2 catalysts. In Fig. 1, we compare the 0.1% Au/SiO_2 and 1% Au/SiO_2 systems. This figure shows that Au NPs are deeply embedded into silica for the 0.1% Au/SiO_2 catalyst (Fig. 1a and b), whereas Au sticks out of the silica surface for the 1.0% Au/SiO_2 sample (Fig. 1c). Probably, the Au solution could have entirely penetrated into the porous silica surface during the reduction step if it were present in a low 0.1% fraction. The contents of Au determined for 1.0% Au/SiO_2 by EDXRF and XPS analyses are shown in Table 1, entry 2. Similar to the 0.1% Au/SiO_2 system, these values do not agree and XPS showed ca. twice as high concentrations as EDXRF. However, in this case, we observed a relative surface Au enrichment. With a larger amount of Au salt used during the reduction process, there is insufficient space within the pores and Au NPs had to spread across the surface.

Over the past few years, a number of techniques have been developed for the production of nanosized metallic particles and their distribution on different carriers [30,31]. The methods in use, based on "the bottom-up" and "the top-down" techniques, still suffer from some disadvantages, including the broad-sized distribution of nanoparticles and their tendency to aggregate or form clumps [30,31]. To minimize these problems, we recently developed a novel innovative method for the formation of bimetallic Pd catalysts [22].

Herein, we tested to determine whether this approach can also be used for other bimetallic systems, in particular, Cu- and Ni-supported Au NPs. After some modifications, fumed silica (f-SiO_2) was also tested as potential target carrier supporting Au NPs. The 1% Au/SiO_2 system was chosen for the intermediate carrier. Accordingly, bimetallic or f-SiO_2 catalysts were synthesized by transfer of Au NPs from 1% Au/SiO_2 to the target carrier. For Cu or Ni, the ingredients were suspended in deionized water, placed in an ultrasound bath, and stirred. Then, SiO_2 was digested. We assumed that the appropriate digesting solvent should fulfill the following requirements: It should digest only the intermediate carrier (i.e., silica), and it must be inert both for the target carrier and metallic nanoparticles. We used 40% aqueous NaOH as a digesting medium. XPS results are shown in Fig. 2. Once again, a comparison of the EDXRF and XPS analyses (Table 1, entries 4 and 5) reveals the surface Au enrichment effect for these new catalysts. The low porosity of Cu and especially Ni determines that, in comparison with SiO_2, a larger fraction of Au NPs are directly available on the surfaces of these catalysts. SEM and TEM analyses prove that Au–Cu or Au–Ni contact is formed in these catalysts (Supplementary material Fig. S3a, S3b, S3c, S3d, S4, S5). However, the residual debris of the original Au/SiO_2 conglomerates can still be detected on the

Table 1
Au content as determined by EDXRF and XPS analyses.

	Catalyst	Au concentration, % (m/m)	
		EDXRF	XPS
1	1.0% Au/SiO_2	0.711 ± 0.042	1.42 ± 0.05
2	0.1% Au/SiO_2	0.092 ± 0.0018	0.04 ± 0.05
3	1.0% Au/f-SiO_2[a]	1.12 ± 0.034	0.2 ± 0.05
4	1.0% Au/Cu	1.18 ± 0.051	7.2 ± 0.1
5	1.0% Au/Ni	1.11 ± 0.030	50.2 ± 0.1

[a] Orisil® 380.

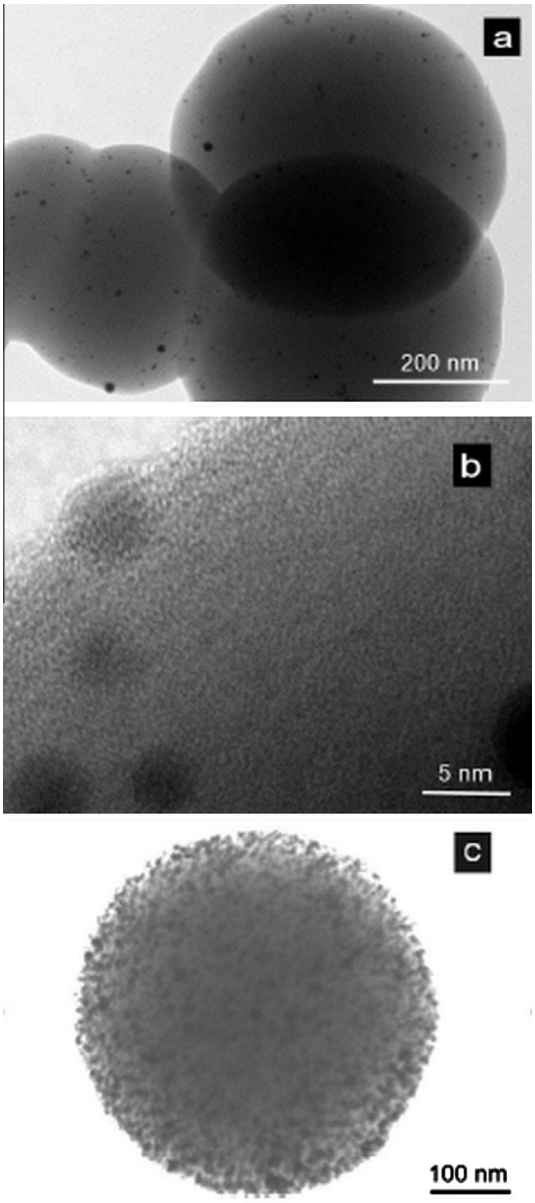

Fig. 1. TEM images of silica supported Au NPs in 0.1% Au/SiO_2 (a, b), 1.0% Au/SiO_2 (c).

metal surface, especially Cu (Supplementary material Fig. S4 and S5).

For the preparation of f-SiO_2 (Orisil)-supported Au NPs, we modified the procedure by preprocessing the intermediate 1% Au/SiO_2 catalyst by sonication with magnesium oxide. Then, the silica digested in aqueous NaOH provided intermediate MgO-supported Au NPs. This material, if sonicated with f-SiO_2, gave a conglomerate from which MgO could be removed in acidic solutions of glacial acetic acid as a digesting solvent. The resulting system is a highly porous silica structure ornamented with Au NPs (for TEM and SEM images see Supplementary material Fig. S6). In this context, the structure resembles that of the 0.1% Au/SiO_2. Further evidence is provided by a comparison of the EDXRF vs. XPS analyses (Table 1, entry 3), which indicates a high discrepancy of the surface and bulk Au concentrations. However, unlike highly monodispersive sol–gel silica, Orisil (which is a polydispersive system), if used as the Au support, also resulted in Au/f-SiO_2 with a much less defined structure. Apart from the small Au clusters below 5 nm, we can, incidentally, find here much larger Au conglomerates.

3.2. Glycerol oxidation in liquid aqueous phase

We assumed that treatment of the concentrated glycerol solutions under mild conditions would potentially be a major advantage for processing waste glycerol. Intuitively, the glycerol concentration that influences the viscosity of a system should strongly control the glycerol *contact with the catalyst* surface. In practice, the catalytic reactions of glycerol in water solutions have been performed previously in a relatively diluted solutions, e.g., in the liquid phase: 0.6 mol/L (mol of glycerol per liter of the reaction mixture, if recalculated using data from the literature; glycerol to H_2O_2 molar ratio amounted to 1:4) [18] or in the vapor phase: Ar/glycerol/H_2O = 5:1:21 [27] or N_2/H_2O/Gly = 46/48/6 [29].

In Table 2, we specified the performance of catalytic Au/SiO_2 systems in the oxidation of glycerol in the diluted liquid phase; 0.2 mol/L glycerol, whereas glycerol to H_2O_2 molar ratio amounted to 1:37. For the new catalysts, i.e., SiO_2-supported Au, both the conversion and selectivity of the process can reach as high as 100% (Table 2, entries 1 and 3), respectively, while in these conditions, the Au/C system provided much lower conversion (Table 2, entry 7). AA (Au/SiO_2) or glycolic acid (GA) and aldehyde (Au/C) were the main products observed for the reactions, respectively. The performance of the Au/C system, typically used for catalytic glycerol oxidation [3], compares well to published data for the 1% Au/C (0.6 mol/L glycerol to H_2O_2 molar ratio 1:4), which provides only slightly higher conversions of ca. 40% [18].

In Table 3, we reported the results of glycerol oxidation where we designed the dilutions amounting to 1.0 mol/L (mol of glycerol per liter of the reaction mixture), while the glycerol/H_2O_2 molar ratio took a value of 1:7. Thus, the dilutions were slightly lower than those usually used in the experiments reported in the literature (0.6 mol/L). For the new catalysts, i.e., SiO_2-supported Au, both the conversion and AA selectivity of the process were slightly lower than those obtained for more diluted solutions (Table 2), reaching ca. 90% (conversion) or more than 85% (AA selectivity), as indicated in Table 3, entries 1 and 3. Also, for the Au/C system (Table 3, entry 4), the conversion is similar to that specified in Table 2, entry 7, i.e., it is similar to that obtained for more diluted glycerol solutions. AA (Au/SiO_2) and glycolic aldehyde (GLAD) (Au/C) were the main products observed for the reactions, respectively.

To test glycerol reactivity in undiluted solutions, we mixed together glycerol and 30% aqueous H_2O_2. This provided a reaction system with 4.5 mol/L glycerol in a reaction mixture in which the glycerol/H_2O_2 molar ratio amounted to 1:1.5. Glycerol was reacted under low temperatures, i.e., below 80 °C. If tested, in undiluted solutions the performance of the 1.0% Au/C system appeared relatively low, not exceeding a conversion of 8%. Glyceric acid (GLA), also a typical product of glycerol oxidation in the presence of C-supported Au NPs, appeared to be the main product of the reaction (Table 4, entry 4). The performance of the SiO_2-supported Au catalysts in the undiluted liquid phase is detailed in Table 4. It is seen that the conversions reached a maximum value of ca. 40% for 0.1% Au/SiO_2 (Table 4, entry 1). The selectivity to AA could reach ca. 80% with a high AA yield for Au/f-SiO_2 (Table 4, entry 3); this appeared now to be the most selective SiO_2-based catalyst. The carbon C-supported system yielded other products under lower selectivities (Table 4, entry 4). In a high-viscosity liquid phase glycerol oxidation to AA, the performance of the 0.1% Au/SiO_2 system is given by an outstanding TON of 26932. A low Au fraction and a high glycerol concentration accompanied by a high conversion rate contribute to this result. This compares with a TON value of 497 for 1% Au/C catalyst, indicating much lower activity. Practically, AA could not be found in the reaction mixture in the 1% Au/C system. It is worth noticing that the f-SiO_2 (Orisil) support appeared to give the highest AA yield in comparison with other SiO_2 systems (Table 4, entries 1, 2, 3).

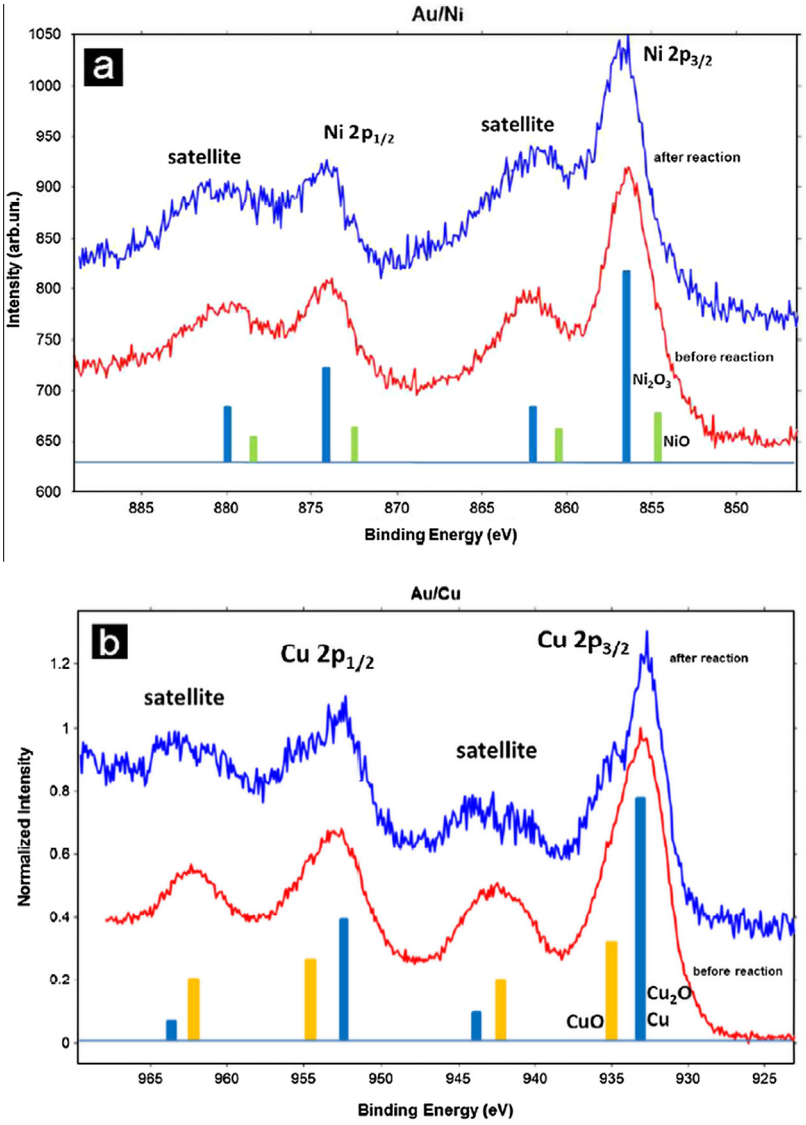

Fig. 2. XPS multiplets of Ni 2p (a) and Cu 2p (b) before and after reaction. The bars represent the contributions from the various oxidation states of Cu and Ni, derived from fitting the data obtained before reaction.

Table 2
Catalytic performance of SiO_2 and C supported Au NPs in diluted glycerol solutions at 80 °C.[a]

	Catalyst	TON[b]	TOF[b] (h^{-1})	Conv. (mol%)	Selectivity to products[c] (mol%)						Yield to acetic acid (%)
					GLAD	GA	TA	AA	FA	OS	
1	0.1% Au/SiO_2	2660	111	100.0	2.2	0	0	90.0	4.9	2.9	90.0
2	1.0% Au/SiO_2	201	8	75.5	1.6	1.8	1.3	84.3	0	11.0	63.7
3	1.0% Au/f-SiO_2[d]	266	11	100	0	0	0	99.3	0	0.7	99.3
4	2.0% Au/SiO_2	125	5	94.3	2.2	0.3	0.4	92.5	0	4.6	87.2
5	5.0% Au/SiO_2	45	2	84.4	1.3	3.2	0	90.9	0	4.6	76.7
6	10.0% Au/SiO_2	23	1	86.0	0	0,7	0	94.0	0	5.3	80.8
7	1.0% Au/C	93	4	35.1	66.7	25.9	0	0	0	7.4	0

[a] 0.2 mol/L of glycerol in the reaction mixture (glycerol/H_2O_2 molar ratio 1:37), 20 mg of catalyst (0.2–20.0 μmol Au), 80 °C, 24 h, 770 rmp.
[b] Turnover number (TON) or turnover frequency (TOF) based on the total gold content in the material.
[c] GLAD – glycolaldehyde, GA – glycolic acid, TA – taratronic acid, AA – acetic acid, FA – formic acid, OS – others.
[d] Fumed silica Orisil® 380

The influence of glycerol dilution in the reaction mixture on the reaction yield and selectivity is shown in Fig. 3. It is clear that the performance of the catalysts significantly decreases with an increase in glycerol concentration. This effect appeared, however, to be less pronounced for the 0.1% Au/SiO_2 system, where the largest conversions were observed independent of glycerol concentration. As could be expected, this effect is also much less distinct for the SiO_2-supported Au then for the C-based catalyst (Table 2, entries 1 vs. 7 and Table 4, entries 1 vs. 4). This can be explained by the substantial difference in wettability of the catalyst supports, i.e., SiO_2 and C, if reacting with the relatively viscous aqueous glycerol solutions.

Table 3
Catalytic performance of SiO_2 and C supported Au NPs in diluted glycerol solutions at 80 °C.[a]

	Catalyst	TON[b]	TOF[b] (h^{-1})	Conv. (mol%)	Selectivity to products[c] (mol%)							Yield to acetic acid (%)
					GLA	GLAD	GA	TA	AA	FA	OS	
1	0.1% Au/SiO_2	12,411	517	87.5	5.5	19.5	0.7	0	54.8	14.5	5.0	48.0
2	1.0% Au/SiO_2	570	24	40.2	0	4.8	4.1	0	79.5	0	11.6	32.0
3	1.0% Au/f-SiO_2[d]	1335	56	94.1	0	0	0.3	0.5	90.6	0	8.6	85.3
4	1.0% Au/C	504	21	35.5	7.3	40.1	10.9	0	0	34.4	7.3	0

[a] 1.0 mol/L of glycerol in the reaction mixture (glycerol/H_2O_2 molar ratio 1:7), 20 mg of catalyst (0.2–2 μmol Au), 80 °C, 24 h, 770 rmp.
[b] Turnover number (TON) or turnover frequency (TOF) based on the total gold content in the material.
[c] GLA – glyceric acid, GLAD – glycolaldehyde, GA – glycolic acid, TA – taratronic acid, AA – acetic acid, FA – formic acid, OS – others.
[d] Fumed silica Orisil® 380

Table 4
Catalytic performance of SiO_2 supported Au NPs in undiluted glycerol solutions at 80 °C.[a]

	Catalyst	TON[b]	TOF[b] (h^{-1})	Conv. (mol%)	Selectivity to products[c] (mol%)							Yield to acetic acid (%)
					GLAD	HPA	GLA	GA	AA	FA	OS	
1	0.1% Au/SiO_2	26,932	1122	40.2	14.2	0	1.5	0	48.6	20.9	14.8	19.5
2	1.0% Au/SiO_2	1606	67	24.0	0	0	0	0	29.9	0	70.1	7.2
3	1.25% Au/f-SiO_2	1875	78	35.0	8.4	3.7	1.9	0	80.3	1.9	3.8	28.1
4	1.0% Au/C	497	21	7.4	12.5	0	31.3	6.2	0	0	50.0	0
5	C	–	–	21.5	21.8	0	3.6	1.8	0	47.3	25.5	0
6	SiO_2	–	–	17.0	29.3	0	4.9	0	0	48.8	17.0	0
7	f-SiO_2	–	–	17.4	33.3	7.1	4.8	0	0	38.1	16.7	0
8	None[a]	–	–	18.7	30.4	15.2	4.4	0	0	39.1	10.9	0

[a] 4.5 mol/L of glycerol in the reaction mixture (glycerol/H_2O_2 molar ratio 1:1.5), 20 mg carrier or catalyst (0.2–2.5 μmol Au), 80 °C, 24 h, 770 rmp.
[b] Turnover number (TON) or turnover frequency (TOF) based on the total gold content in the material.
[c] GLA – glyceric acid, GA – glycolic acid, GLAD – glycolaldehyde, HPA – hydroxypyruvic acid, AA – acetic acid, FA – formic acid, OS – others.

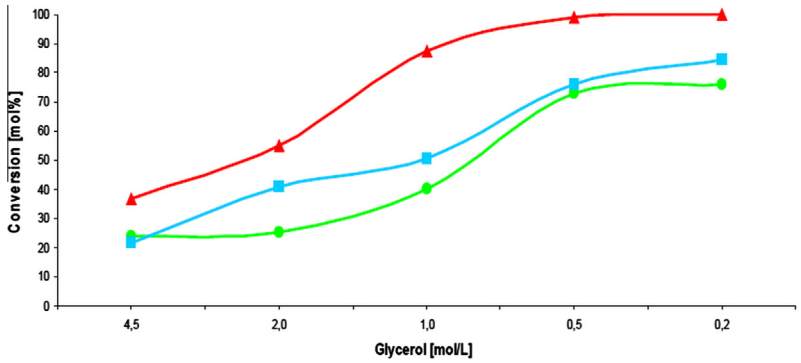

Fig. 3. Conversion of glycerol vs. glycerol concentration, 0.1% Au/SiO_2 (▲), 1.0% Au/SiO_2 (●) and 5.0% Au/SiO_2 (■). Reaction conditions: 20 mg of catalyst (0.2–10.0 μmol Au), 80 °C, 24 h, 770 rpm.

Additionally, we performed blind experiments without Au NPs to carefully test glycerol reactivity in the systems investigated (Table 4, entries 5–8). It is interesting that glycerol conversion can reach about 20% in such conditions, but the reaction products appeared to be completely different than those formed in the presence of Au NPs (Table 4, entries 1–4). Non-catalytic and quasi-homogeneous glycerol oxidation in aerobic conditions was investigated recently by Skrzynska et al. [17], who also investigated oxidation in non-catalytic glycerol solutions (but basic) at high temperatures and similarly noted different reaction paths for catalytic and non-catalytic processes. An interesting fact is that, in our systems of undiluted solutions, a conversion can be higher without Au (Table 4, entries 5–8) than for C-supported Au NPs (Table 4, entry 4). However, completely different products were formed in these processes, i.e., formic acid for Au free, vs. AA for SiO_2-supported Au (Table 4, entries 1–3), or C_3 oxygenates for C-supported Au (Table 4, entry 4).

In non-diluted glycerol solutions, the selectivity to AA can be increased under the addition of acetonitrile (Table 5). It is worth mentioning that the addition of acetonitrile allowed us to decrease the reaction temperature to 60 °C vs. 80 °C in acetonitrile-free conditions; however, a nominal glycerol concentration after the addition of acetonitrile was lower 2.7 mol/L vs. ca. 4.5 mol/L in the acetonitrile-free conditions. Moreover, the addition of acetonitrile (Table 5, entries 2 (+) and 4 (−)) also increases the selectivity of the AA formation for the f-SiO_2-supported Au system.

Paradoxically, independent of glycerol dilution, higher conversion and AA selectivities were observed for 0.1% Au NPs (Table 2, entry 1 or Table 4, entry 1) and not for the catalyst containing higher Au contents 1–10% (Table 2, entries 2 and 4–6 or Table 4, entries 1 and 3). This seems to prove a heterogeneous character of the process and the importance of the specific highly porous structure of the 0.1% Au/SiO_2 system, where Au is placed in pores. This is discussed in Section 3.1.

It has been recently reported that Au/Cu nanoparticles can form an interesting catalyst for the oxidation of various alcohols [23]. Thus, we prepared the related nano-Au/Cu and nano-Au/Ni catalysts. The catalytic performance of these novel Cu- and

Table 5
Catalytic performance of SiO_2 supported Au NPs in undiluted glycerol solutions at 60 °C with (+) and without (−) acetonitrile.

	Catalyst	CH_3CN	Conv. (mol%)	Selectivity to products[c] (mol%)							Yield to acetic acid (%)
				GLA	GA	GLAD	HPA	AA	FA	OS	
1	1.0% Au/SiO_2	+[a]	40.2	0	0	0	0	99.5	0	0.5	40.0
2	1.25% $Au/f\text{-}SiO_2$	+[a]	23.6	0	1.6	0	0	88.2	4.8	5.4	20.9
3	1.0% Au/SiO_2	−[b]	14.9	0	2.9	0	0	91.4	0	5.7	13.6
4	1.25% $Au/f\text{-}SiO_2$	−[b]	33.7	7.9	0	21.6	14.8	0.7	41.3	13.7	0.3

[a] 2.7 mol/L of glycerol in the reaction mixture (glycerol/H_2O_2/acetonitrile molar ratio 1:1.5:2.8), 20 mg catalyst (2.0–2.5 μmol Au), 60 °C, 24 h, 770 rmp.
[b] Glycerol: 4.5 mol/L (glycerol/H_2O_2 molar ratio 1:1.5).
[c] GLA – glyceric acid, GA – glycolic acid, GLAD – glycolaldehyde, HPA – hydroxypyruvic acid, AA – acetic acid, FA – formic acid, OS – others.

Table 6
Catalytic performance of bimetallic Cu or Ni supported Au NPs.[a]

	Catalyst	Conv. (mol%)	TON[b]	TOF[b] (h^{-1})	Selectivity to products[c] (mol%)							Yield to acetic acid (%)
					HPA	GLA	GLAD	GA	AA	FA	OS	
1	1.0% Au/Cu	41.2	2762	115	5.0	0	0	3.6	85.7	1.4	4.3	35.3
2	1.0% Au/Ni	39.6	2657	111	0	7.6	0	0	80.2	9.1	3.1	31.8
3	Cu	40.5	–	–	0	27.9	16.2	2.2	3.4	19.1	31.2	1.4
4	Ni	35.7	–	–	28.8	13.5	0	0	3.6	18.0	36.1	1.3

[a] 4.5 mol/L of glycerol in the reaction mixture (glycerol/H_2O_2 molar ratio 1:1.5), 20 mg carrier or catalyst (0.2–2.5 μmol Au), 80 °C, 24 h, 770 rmp.
[b] Turnover number based on the total gold content in the material – Turnover frequency based on the total gold content in the material.
[c] GLA – glyceric acid, GA – glycolic acid, GLAD – glycolaldehyde, HPA – hydroxypyruvic acid, AA – acetic acid, FA – formic acid, OS – others.

Table 7
Catalytic performance of 0.1% Au/SiO_2 at room temperature,[a] if enhanced by surfactant addition.

	Surfactant	Conv. (mol%)	TON[b]	TOF[b] (h^{-1})	Selectivity to products[c] (mol%)		Yield to acetic acid (%)
					AA	OS	
1	Sulforokanol	8.8	5876.1	244.8	68.8	31.2	6.0
2	Triton X-100	7.9	5312.6	221.4	88.4	11.6	7.0
3	PEG 400	9.4	6278.5	261.6	80.6	19.4	7.6
4	None	4.7	3192.9	133.0	30.2	69.8	1.4

[a] 4.5 mol/L of glycerol in the reaction mixture (glycerol/H_2O_2 molar ratio 1:1.5) surfactant (0.05 wt.%), 25 °C, 24 h, 770 rpm.
[b] Turnover number (TON) or turnover frequency (TOF) based on the total gold content in the material.
[c] AA – acetic acid, OS – others.

Ni-supported Au catalysts in glycerol oxidation in non-diluted solutions is given in Table 6. Basically, the results are slightly better than those obtained for the similar Au/SiO_2 system (Table 4, entry 2). Maximal TON for the bimetallic Au/Cu system amounted to 2762, while high selectivity toward a formation of the C_2 products was observed. In particular, AA was the main product, while a formation of glyceric acid (GLA) was not observed. Similar to the SiO_2 support, we performed a blind test performing oxidation on Cu or Ni (Table 6, entries 3 or 4). This provided similar conversions to the Au-catalyzed reaction (Table 6, entries 1 or 2) but with much lower selectivities. Moreover, other products were yielded then those obtained in the catalytic process.

Although Au supported on Cu or Ni gave repeatable oxidation results, these catalysts appeared to be consumed during the reaction. After about three hours, we observed that the reaction mixture color changed to green for nickel or blue for copper, which suggested oxidation of Cu or Ni supports accompanied by their dissolution. In order to check the amount of released metal, we determined the concentrations of Cu and Ni in the reaction mixture shown in Fig. 2 and Table S2 (Supplementary material). Thus, a process of metal digestion accompanied oxidation to carboxylic acids, which in the presence of H_2O_2, possibly through peroxyacids, can oxidize the supporting metals and digest them into the solution. A similar effect was described earlier [33]. An analysis of the Cu redox behavior indicates that this can be a complex process that includes Cu oxidation and comproportionation [31,32].

In the Au/Ni bimetallic catalyst, a structure of the Ni 2p XPS multiplet indicates Ni_2O_3 as the main component with a small amount of NiO (Fig. 2a). The reaction did not change this. The situation is similar for the Cu support where two oxidation states can be detected: a relatively weak contribution from CuO represented within the Cu $2p_{3/2}$ component by the line with binding energy of about 935 eV, and the characteristic broad satellite structure situated in the region 940–945 eV (Fig. 2b). Their counterparts are visible within the Cu $2p_{1/2}$ line. The dominant contribution comes from either Cu_2O or Cu. The positions of the lines for metallic Cu and oxide I are roughly the same [34], and we cannot distinguish between these two oxidation states. The reaction led to a slight change in the ratio between two oxidation states as it partly reduced CuO. Its contribution, as derived from fitting, decreased from about 46% to 37%.

Thus far, the results of the exhaustive oxidation of glycerol indicated that catalyst availability is of major importance for the observed performance of the system. Below, we report the results of the experiments in which we tested possible applications of the surfactants to improve this feature (Table 7). We observed that a conversion and the yield of AA can be almost doubled at room temperature when Sulforoktanol, PEG 400, or Triton X-100 were used as surfactants.

In a series of additional experiments, we tested the catalytic stability of the SiO_2-supported systems during glycerol oxidation in the liquid phase. The catalyst separation was facilitated via

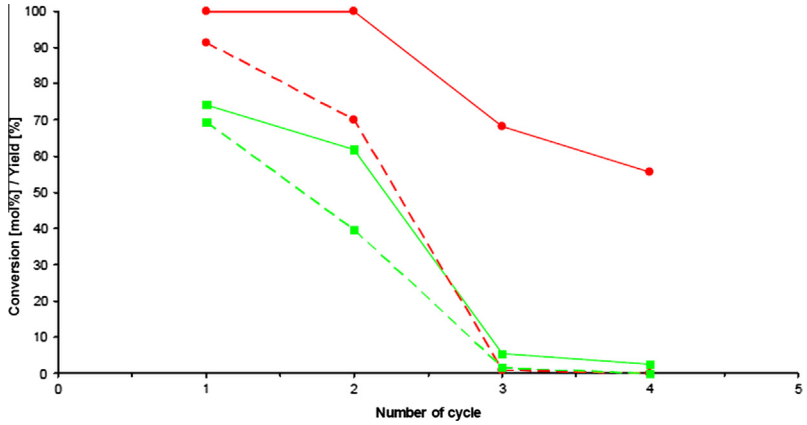

Fig. 4. Catalyst recycling: the change of glycerol conversion (solid lines) and yield to acetic acid (dotted lines) for 0.1% Au/SiO_2 (●) and 1.0% Au/SiO_2 (■) with recycle number. Reaction conditions: glycerol concentration 0.2 mol/L of glycerol concentration in reaction mixture (glycerol/H_2O_2 molar ratio 1:37), 20 mg of catalyst (0.2–2.0 μmol Au), 80 °C, 24 h, 770 rpm.

centrifuge assistance. A facile recycling method involved catalyst filtration, washing, and drying. The results of these experiments are detailed in Fig. 4. Catalyst reusability dependent on the individual Au/SiO_2 system appeared to be the best for the 0.1% Au/SiO_2 system. In this case, the initial 100% conversion was observed in 2 cycles and decreases to ca. 60% after 4 cycles. However, the AA yield decreased already in the second cycle to ca. 70%, while the Au content after 4 cycles decreased to 25%–10% (EDXRF) of the initial Au content in the catalyst.

4. Conclusions

We assumed that a high catalyst reactivity accompanied by the support wettability and availability should be of major importance in viscous glycerol solutions. Thus, we investigated as a potential catalyst for glycerol processing SiO_2-supported Au NPs that should be compatible with the polar reactant, oxidant, and solvent, i.e., glycerol, H_2O_2, and H_2O, respectively. Such a catalyst has not been tested previously in glycerol processing. In fact, tested Au/SiO_2 systems appeared more reactive than Au/C systems. Since Au/Cu nanoparticles have been recently reported as an interesting catalyst for the oxidation of various alcohols, we prepared bimetallic catalysts here. We performed a broad series of experiments in order to compare Au/SiO_2, Au/Cu, and Au/Ni systems, some of which were prepared by the innovative nano-Au transfer method. Bimetallic Au/Cu and Au/Ni catalysts appeared relatively efficient; however, they were destroyed during the reaction by the Cu or Ni leaching effect.

We observed that, within the complex network of possible reactions, a process of deep glycerol oxidation proceeded on Au/SiO_2 catalysts preferentially to acetic acid. The selectivity of glycerol oxidation to C_3 products was investigated thoroughly. It is not a coincidence, because only C_3 oxygenates can form the single carbonous products of glycerol processing, while any oxidation to C_2 must also yield the C_1 oxygenate ($C_3 \rightarrow C_2 + C_1$). This means that, although the process can be fully selective, we obtain at least two products.

Thus, the reactivity to C_3 products has been well described, in contrast to the C_1 and C_2 products. Herein, we described the systems providing high selectivity to acetic acid, the C_2 glycerol oxygenate. High conversions (100%) and acetic acid yields (90–99%) were observed for the best catalysts in the diluted aqueous glycerol solutions. Although in a relatively viscous liquid phase these values decreased to ca. 40% and 20%, the addition of acetonitrile could improve the acetic acid yield to ca. 40%, while surfactants were found to be capable of a many-fold enhancement of the catalyst activity. However, this was relatively low at the room temperature highly viscous liquid phase.

In summary, SiO_2-supported Au NPs can form an interesting catalytic system for deep selective glycerol oxidation to acetic acid in undiluted viscous liquid solutions. This seems especially interesting for the processing of glycerol wastes.

Acknowledgments

The research was co-financed by the National Research and Development Center (NCBiR) under Grant ORGANOMET no: PBS2/A5/40/2014 Maciej Kapkowski and Mateusz Korzec appreciates the support of the Doktoris fellowships.

Appendix A. Supplementary material

Supplementary data associated with this article can be found, in the online version, at http://dx.doi.org/10.1016/j.jcat.2014.08.003.

References

[1] C.J. Li, B.M. Trost, PNAS 105 (2008) 13197.
[2] N. Dimitratos, J.A. Lopez-Sanchez, G.J. Hutchings, Top. Catal. 52 (2009) 258.
[3] M. Besson, P. Gallezot, C. Pinel, Chem. Rev. 114 (2014) 1827.
[4] C.H. Zhou, H. Zhao, D.S. Tong, L.M. Wu, W.H. Yu, Catal. Rev. – Sci. Eng. 55 (2013) 369.
[5] S. Philippe, P. Karine (Eds.), Nanomaterials in Catalysis Introduction, in: S. Philippe, P. Karine (Eds.), Concepts in Nanocatalysis, Viley-VCH, Weinheim, 2013, pp. 1–5.
[6] Y. Zhang, X. Cui, F. Shi, Y. Deng, Chem. Rev. 112 (2012) 2467.
[7] C.D. Pina, E. Falletta, M. Rossi, Chem. Soc. Rev. 41 (2012) 350.
[8] M.D. Hughes, Y.J. Xu, P. Jenkins, P. Mcmorn, P. Landon, D.I. Enache, F. Carley, G.A. Attard, G.J. Hutchings, F. King, E.H. Stitt, P. Johnston, K. Griffin, C.J. Kiely, Nature 437 (2005) 1132.
[9] A.S.K. Hashmi, G.J. Hutchings, Angew. Chem. Int. Ed. 45 (2006) 7896.
[10] P. Bujak, P. Bartczak, J. Polanski, J. Catal. 295 (2012) 15–21.
[11] S. Carrettin, P. McMorn, P. Johnston, K. Griffin, G.J. Hutchings, Chem. Commun. 7 (2002) 696.
[12] S. Carrettin, P. McMorn, P. Johnston, K. Griffin, C.J. Kiely, G.J. Hutchings, Phys. Chem. Chem. Phys. 5 (2003) 1329.
[13] R. Schoevaart, T. Kieboom, Top. Catal. 27 (2004) 1.
[14] J. Ma, W. Yu, M. Wang, X. Jia, F. Lu, J. Xu, Chin. J. Catal. 34 (2013) 492–507.
[15] S. Gil, M. Marchena, C.M. Fernández, L. Sánchez-Silva, A. Romero, J. Luís Valverde, Appl. Catal. A 450 (2013) 189.
[16] B. Katryniok, H. Kimura, E. Skrzyńska, J.S. Girardon, P. Fongarland, M. Capron, R. Ducoulombier, N. Mimura, S. Paul, F. Dumeignil, Green Chem. 13 (2011) 1960.
[17] E. Skrzyńska, J. Ftouni, J.S. Girardon, M. Capron, L. Jalowiecki-Duhamel, J.F. Paul, F. Dumeignil, ChemSusChem 5 (2012) 2065–2078.
[18] M. Sankar, N. Dimitratos, D.W. Knight, A.F. Carley, R. Tiruvalam, C.J. Kiely, D. Thomas, G.J. Hutchings, ChemSusChem 2 (2009) 1145.
[19] A. Villa, G.M. Veith, L. Prati, Angew. Chem. Int. Ed. 49 (2010) 4499.

[20] S. Gil, L. Muñoz, L. Sánchez-Silva, A. Romero, J.L. Valverde, Chem. Eng. J. 172 (2011) 418–429.
[21] A. Behr, J. Eilting, K. Irawadi, J. Leschinski, F. Lindner, Green Chem. 10 (2008) 13.
[22] M. Korzec, P. Bartczak, A. Niemczyk, J. Szade, M. Kapkowski, P. Zenderowska, K. Balin, J. Lelątko, J. Polanski, J. Catal. 313 (2014) 1.
[23] Y. Sugano, Y. Shiraishi, D. Tsukamoto, S. Ichikawa, S. Tanaka, T. Hirai, Angew. Chem. Int. Ed. 52 (2013) 5295.
[24] K.S. Rao, J. Colloid Interface Sci. 289 (2005) 125.
[25] H. Okudera, A. Hozumi, Thin Solid Films 434 (2003) 62.
[26] M. Pagliaro, M. Rossi, The Future of Glycerol, second ed., RSC Publishing Cambridge, 2010.
[27] M. Massa, A. Andersson, E. Finocchio, G. Busca, J. Catal. 307 (2013) 170.
[28] B. Katryniok, S. Paul, F. Dumeignil, ACS Catal. 3 (2013) 1819.
[29] J. Deleplanque, J.L. Dubois, J.F. Devaux, W. Ueda, Catal. Today 157 (2010) 351.
[30] H. Skaff, T. Emrick, in: V. Rotello (Ed.), Nanoparticles: Building Blocks for Nanotechnology, Springer Science and Business Media Inc., New York, 2004, p. 32.
[31] N.H. Nguyen, V. Percec, J. Polym. Sci., Part A: Polym. Chem. 49 (2011) 4241.
[32] K.L. Chavez, D.W. Hess, J. Electrochem. Soc. 148 (2001) 640.
[33] S. Sahu, N.C. Kauri, M. Kundu, Braz. J. Chem. Eng. 28 (2011) 251.
[34] M.C. Biesinger, L.W.M. Lau, A.R. Gerson, R.St.C. Smart, Appl. Surf. Sci. 257 (2010) 887.